

Unraveling the fluctuations of animal motor activity

C. Anteneodo¹ and D. R. Chialvo²

¹*Departamento de Física, PUC-Rio, and National Institute of Science and Technology for Complex Systems, Rua Marquês de São Vicente 225, CEP 22453-900 RJ, Rio de Janeiro, Brazil*

²*Department of Physiology, Feinberg Medical School, Northwestern University, 303 East Chicago Ave., Chicago, Illinois 60611, USA*

(Received 5 June 2009; accepted 31 July 2009; published online 25 August 2009)

Human and animal behavior exhibits power law correlations whose origin is controversial. In this work, the spontaneous motion of laboratory rodents was recorded during several days. It is found that animal motion is scale-free and that the scaling is introduced by the inactivity pauses both by its length as well as by its specific ordering. Furthermore, the scaling is also demonstrable in the rates of event's occurrence. A comparison with related results in humans is made and candidate models are discussed to provide clues for the origin of such dynamics. © 2009 American Institute of Physics. [DOI: 10.1063/1.3211189]

Recent findings of heavy tailed distributions in the patterns of human activity reemphasized our poor understanding on the mechanisms responsible for such type of dynamics. To shed light on the most significant features of these fluctuations, the problem is here oversimplified by studying a much elementary system: the spontaneous motion of rodents recorded during several days. The analysis of the animal motion reveals a robust scaling not only in univariate distributions, comparable with the results previously reported in humans, but also in its correlation structure. It is shown that the most relevant features of the experimental results can be replicated by the statistics of the activation-threshold model proposed in another context by Davidsen and Schuster. It constitutes an alternative mechanism to queuing, cascading, and nonhomogeneous processes, currently contemplated as candidates to account for the statistics of diverse human activities, but that seem not suitable for motion patterns.

I. INTRODUCTION

Much debate has been dedicated recently to the dynamics of human activity, including the temporal patterns of disparate activities such as letters^{1,2} or e-mail correspondence,¹⁻⁵ visiting a library, trading in a stock market, accessing the web,¹ or initiating a movement.⁶⁻⁸ The interest in the topic is triggered by the existence of a seemingly common feature, namely, the heavy tails of the waiting and interevent time distributions.

There are two fundamental issues in this problem. First, it is still unclear which is the precise character of the heavy tails, whether they are power law, log normal, or something else. Second, there is no agreement on the mechanisms generating such statistics. The simplest example probably is the temporal spacing between -even inconsequential- motor activities, which appears to be scale-free.⁶⁻⁹ Despite these recent efforts the mechanisms behind such statistical behavior are not understood yet. This lack of plausible models calls for alternatives which can be helpful to identify the mechanisms at work.

To that end, it may be advantageous to simplify the process by eliminating numerous cognitive factors present in all experiments with human subjects. This can be done by analyzing more elementary processes such as records of long-term spontaneous motor activity of laboratory animals, as recently reported in mice experiments.⁹

In the present work, the activity of rats was recorded during several days. Each, even minute, movement of the animal was detected and the experimental data series analyzed from the perspective of a point process.

The paper is organized as follows. In Sec. II the experimental details are described. Section III contains the statistical analysis, first for the interevent times, then for the rates of motion events, and finally for the variance of counts. Section IV describes an activation-threshold model which is able to replicate the most relevant experimental observations. Finally, Sec. V closes the paper with a discussion of further implications of the present results.

II. EXPERIMENTAL SETTING AND DATA RECORDING

Six male 4-month-old Wistar rats were kept in a sound-proof room temperature ($\sim 20-22$ °C) and humidity ($\sim 50\%-80\%$) conditioned chambers. The animals were individually isolated in transparent cages of $25 \times 25 \times 12$ cm³ with food pellets and tap water ad libitum. Note that the cage's dimensions correspond to those used for housing adult laboratory rats. It is well known that rodents prefer relatively small environments and are stressed by relatively large open spaces. They were exposed to a 24-h cycle of light-dark conditions: cycles of 12 h of light (fluorescent lamps with intensity of 300 lx) and 12 h of darkness (dim red light with intensity less than 0.1 lx).¹⁰

Each animal's movement was monitored with infrared activity meters, able to scan each rodent housing cage and to report, at a frequency of 1 Hz, animal movements even in absence of locomotion. Given the sensor's sensitivity, the detection includes even minute head motion, grooming, etc. Then, the raw data are a binary sequence composed of 1's

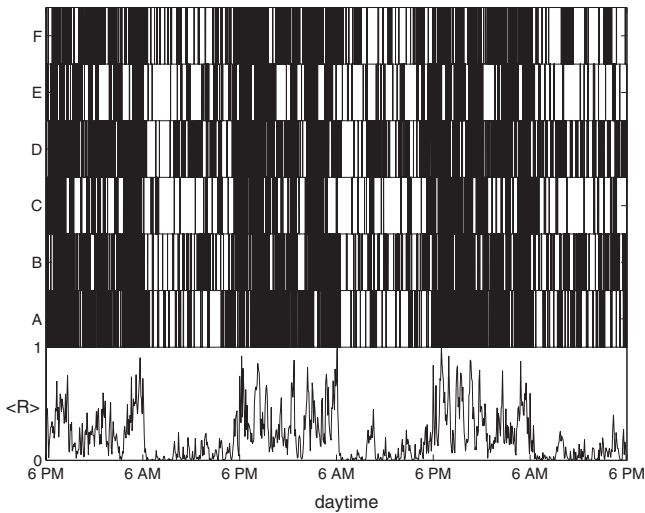


FIG. 1. Three day activity plot obtained from six laboratory animals (“A”–“F”) exposed to a cycle of 12 h of light (6 a.m.–6 p.m.) and darkness (6 p.m.–6 a.m.), individually housed and continuously monitored by an infrared device scanning the field at a rate of 1 Hz. The bottom time series depicts the group average activity $\langle R \rangle$ computed with a binwidth of 1 min and normalized.

(whenever the animal moves) and 0’s (during immobility). An example of the recording for the first 3 days is plotted in Fig. 1, where changes from activity to immobility, and vice versa, are marked by a vertical bar with a resolution of 1 s. In the bottom plot of Fig. 1, we also show the group average of the activity rate R , which is a coarse graining of the raw data, exhibiting the well known circadian rhythmicity.

As discussed in Sec. I, our interest here focuses exclusively on understanding the dynamics of the irregular fluctuations and not on the circadian periodicity.

III. STATISTICAL PROPERTIES

The spatial and temporal resolution of our experimental setting is such that from the original (binary) data recorded, we can precisely estimate the duration of motion (sequences of consecutive 1’s) and immobility (sequences of consecutive 0’s) episodes. Thus, the animal motor activity can be interpreted as a point process where the beginning of a motion event i occurs at a definite discrete time t_i . The point process can be then specified by the sequence of event times t_i or, alternatively, by the series of increments (or interevent intervals) $\tau_i = t_{i+1} - t_i$. A typical plot of the τ -series is presented in Fig. 2. It is evident that beyond the circadian rhythmicity, clustering or bursts of activity occur.

In order to characterize this point process we will first consider the τ -series, obtaining its distribution and correlation structure. Next, rates of events will be inspected. Finally, the statistics of event’s counts¹¹ as a function of observation times will be described.

A. Interevent intervals

Figure 3 shows the estimation of the probability density $P(\tau)$ through the relative frequency of occurrence of interevent times and durations. It was computed over the 9-day binary sequence of activity for each one of the six animals.

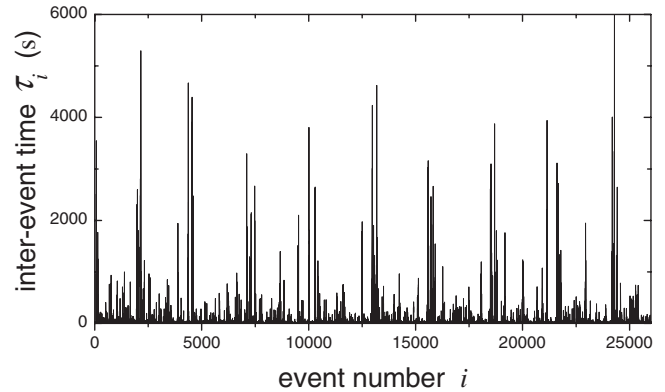


FIG. 2. Interevent time τ_i as a function of the event number i (data from animal A).

We have overimposed the plots from all the animals to demonstrate the robustness of the results. It can be clearly seen that from few seconds to several thousands seconds (about 1 h), the distribution of interevent times decays as a power law (with exponent μ falling within the interval of 1.75 ± 0.05 for all six animals).

In contrast, the distribution of the duration of motion episodes does possess a characteristic time scale (see Fig. 3). It can be described by a superposition of two exponentials with characteristic times of the order of 1 and 4 s, close to the smaller data resolution and to the average duration of motion episodes, respectively. Let us note that for human (arm) motor activity data, instead of two exponentials, a stretched exponential fit was reported.^{7,9}

Meanwhile, quiescence intervals are also power law distributed with exponent μ . Because motion intervals are in average much shorter than quiet ones, then, the statistics of interevent times is mainly dominated by that of immobility

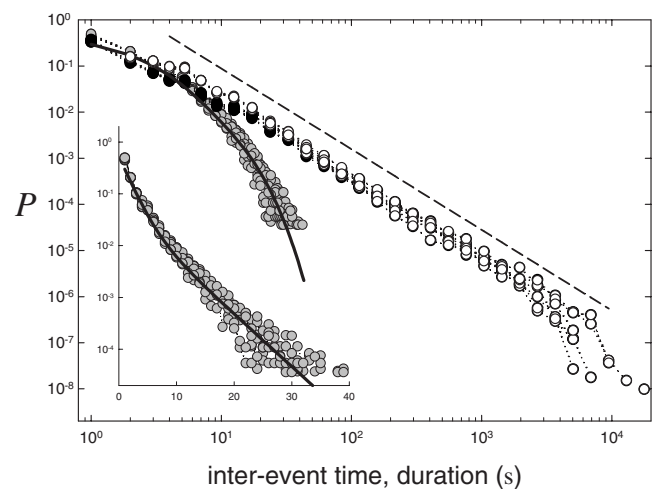


FIG. 3. Normalized distributions of interevent times τ (empty symbols), duration of motion episodes (gray symbols), and duration of immobility periods (black symbols) computed from 9 days of continuous recording. Symbols joined by dotted lines correspond to the results from each one of the six animals. The solid lines correspond to a double exponential fit (with characteristic times of the order of 1 and 4 s). The dashed line, drawn for comparison, has a slope of -1.75 . Inset: representation of the distribution of motion episodes in log-linear scale. Statistics computed individually for each of the six animals and plotted overimposed.

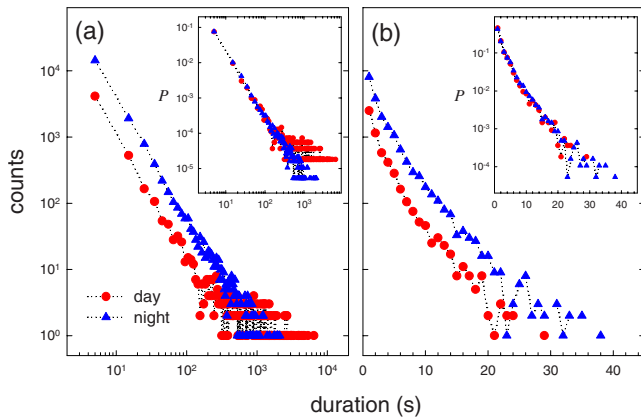


FIG. 4. (Color online) Distributions of duration of (a) immobility and (b) mobility episodes at day (circles) and night (triangles) for animal A. Insets: normalized distributions of the same data. A linear binning was used to emphasize the tail fluctuations.

periods, in particular, sharing the same power-law decay. Hence, discrepancies between both histograms are evident for small time intervals only (see Fig. 3). For comparison, let us note that for the power-law exponent of the cumulative histogram of inactivity periods of human (arm) motor activity, the values 0.92 (control) and 0.74 (depressed individuals), with about 10% relative error, have been reported.⁷ Meanwhile, recent experiments with wild and mutant mice give exponents of 0.93 and 0.84, respectively.⁹

Daytime and nighttime fluctuations were also analyzed separately. The results are illustrated in Fig. 4 with the histogram of duration of mobility and immobility sequences for a representative animal. The figure shows that (i) activity episodes follow the same exponential statistics at day and night periods, (ii) the interevent times statistics has a good agreement between both periods up to ~ 10 – 20 min, and a discrepancy seems to occur for longer times, although the statistics at that range is dominated by a few events, as it is always the case for heavy tails. To emphasize the small number of counts in the tails, the figure shows also the histograms in the insets. In addition this figure shows that the main difference between day and night statistic is a shift in the curves by a constant factor (of about 4). In other words, even though the animals are more active at night, the statistics of duration and intervals are similar. The agreement between day and nighttime results up to several hundred seconds, despite the statistical fluctuations for longer times, suggests a single scaling mechanism.

To assess correlations between consecutive motion episodes, first we computed the spectral density of τ . The results displayed in Fig. 5 show that the interevent intervals are not independent, exhibiting long-range correlations. Therefore, the stochastic point process of motor activity cannot be considered a renewal one. Because of the relatively small value of the exponent of the τ power spectrum, we computed also that of the increments, which helps to confirm that it is not white noise. Although not shown, we verified also that motion and quiescent intervals are anticorrelated.

Correlations of day and night data were also computed separately. For all animals, a similar behavior to those exhib-

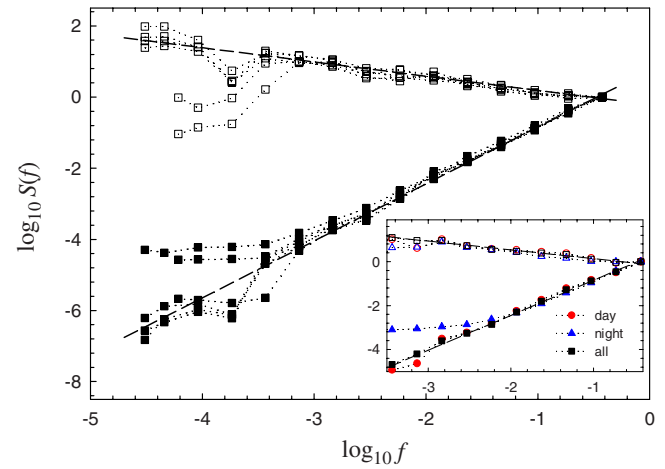


FIG. 5. (Color online) Long-range correlations of interevent times. Log-log plot of the power spectra for the six series of interevent intervals (open symbols) and of their increments (filled symbols). Data were logarithmically binned. Here f is the inverse of the instantaneous period between consecutive events. Dotted lines are a guide to the eyes. Dashed lines with slopes of -0.4 and 1.6 are drawn for comparison. Notice that $\alpha=0.4$ and $\beta=1.6$ verify $\alpha=2-\beta$. Inset: separate analysis of day and night periods for animal B. Spectra were normalized for better comparison.

ited for the whole data set is observed for $f > 10^{-2}$, corresponding to at least 100 events, as illustrated in the inset of Fig. 5.

B. Local rates

Due to the presence of correlations in interevent times, local rate analysis may provide additional nonredundant information. A typical plot of the cumulative number of events $\mathcal{N}(t)=m$ versus time $t=\sum_{n=1}^m \tau_n$ is shown in Fig. 6(a). One observes that the local rate (local slope) is not constant as in standard Poisson processes, rather there is an irregular rapidly changing component superimposed to the circadian modulation.

In order to depict more precisely rate inhomogeneities, we estimated local rates as follows. By dividing the whole observation time interval in W (nonoverlapping) uniform windows of length T and counting the number of events N_n in each time window n , one obtains the series of counts. The local rate R_n is the ratio N_n/T . In the scale of half-day, one observes two characteristic mean rates associated with the half-periods of low and high activity levels. However, for shorter time windows T , rates fluctuate in time, as exhibited in the inset of panel 6(a). However, the distribution of rates is not simply bimodal but scale-free, as displayed in Fig. 6(b). It follows a power law (with exponent $\gamma \approx 0.75$) with exponential cutoff. Furthermore, rate densities computed at various time window lengths (from 128 to 1024 s) show finite size effects, demonstrated by the good collapse obtained for all curves by an ansatz of the form $P(R) \propto f(RT^\gamma)/R^\gamma$, where $f(x)$ goes to a constant value for small x and decays exponentially for large x . The separate analysis of day and night data [panel 6(c)] reveals the same scaling function describing both statistics, although the value of the exponent γ is different for each case.

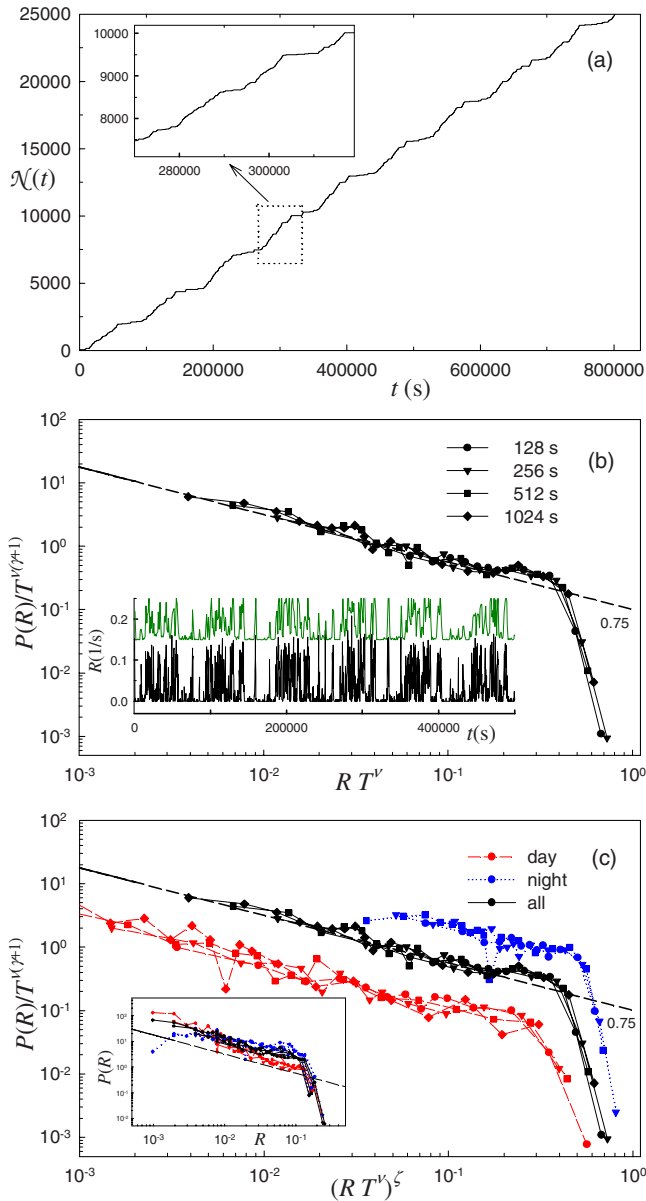


FIG. 6. (Color online) (a) Cumulative number of events as a function of time. A zoom is displayed in the inset. (b) Scaled distribution of local rates R computed over nonoverlapping time windows of lengths T indicated on the figure. Data collapse is obtained for $\nu=0.2$, and $\gamma=0.75$. Inset: time series of local rates R for time window length of 256 (black) and 1024 s (green), vertically shifted for better visualization. (c) Separate analysis of nighttime and daytime data: $\nu=0.2$, $\zeta=0.75/\gamma$ with $\gamma\approx 0.5$ (daytime) 1.5 (nighttime). Inset: unscaled plots of the same data. Note the absence of any characteristic scale for the local rates demonstrated by the fact that the three calculated rate densities follow a truncated scale-free distribution. The dashed lines with slope $\gamma=0.75$ are drawn for comparison. All data are from animal A.

Nonhomogeneous Poisson processes with (uncorrelated) stochastic rates have been considered to explain the emergence of scaling in the statistics of interevent times (see, for instance, Ref. 12). Since in the present case the interevent intervals are not independent, such inhomogeneous Poisson processes can be excluded as responsible for this dynamics.

To estimate rate's linear correlations, we performed a spectral analysis of the time series of increments $I_n=R_n-R_{n-1}$. Figure 7 is a log-log plot of its power spectrum $S(f)$.

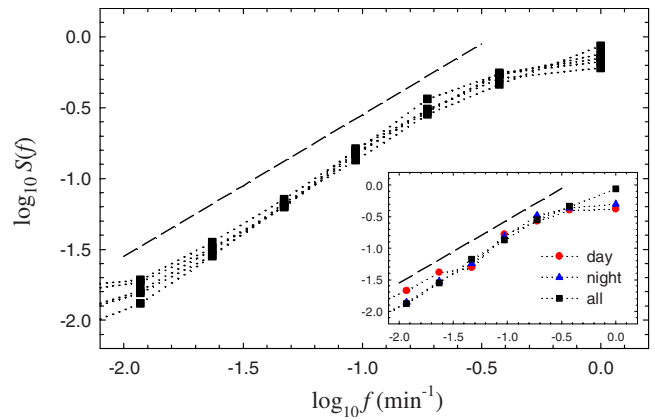


FIG. 7. (Color online) Long-range anticorrelations in the increments I_n of activity rates R_n computed over 1-min windows. Log-log plot of the power spectra for the six I time series (symbols). The dashed line with slope $\beta=1$ indicates the correlations expected for pink noise (data from six animals). Inset: the same analysis performed separately for day and nighttime data of animal F. (In all cases spectra were log binned and normalized for better comparison.)

It is approximately linear on a wide range of biologically relevant temporal scales implying that $S(f)\sim f^\beta$ with $\beta\sim 1$. Since $\beta>0$, consecutive values of the process I are negatively correlated, meaning that increases in activity are, on the average, more likely to be followed by decreases and vice versa. The same applies for day and night separate data, as shown in the inset of Fig. 7. Shuffling the time series of increments yields white noise. Recalling that R is the integration of I , then the spectral density of the original R time series decays as $1/f^\alpha$ with $\alpha=2-\beta$.¹³

C. Variance of counts

Common measures for detecting correlations in sequences of counts are the Fano (FF) and Allan (AF) factors.¹¹ The former is the ratio of the variance to the mean of the number of events in each time window, $FF=(\langle[N_k]^2\rangle-\langle N_k\rangle^2)/\langle N_k\rangle$, an index of dispersion of counts. The latter quantifies the discrepancy of counts between consecutive windows, being $AF=(\langle[N_{k+1}-N_k]^2\rangle)/(2\langle N_k\rangle)$. Although related, they reflect different features; therefore we kept track of both of them.

In Fig. 8, the two factors are plotted as a function of the length of the counting time window T . There is a range where they increase as T^d . The exponent of FF is $d\in[0.65,0.73]$ (that is $d\approx\mu-1$ within error bars) for the six laboratory animals, while that of AF is about 0.1 higher. The discrepancy may be due to the fact that $FF(AF)$ tends to the power law from above (below). Shuffling the series of interevent intervals modifies both factors mostly by reducing the upper bound of the power-law scaling region. This indicates that the scaling properties are partially due to the distribution of interevent intervals itself, but also that longer range correlations are associated with the specific ordering of the intervals.

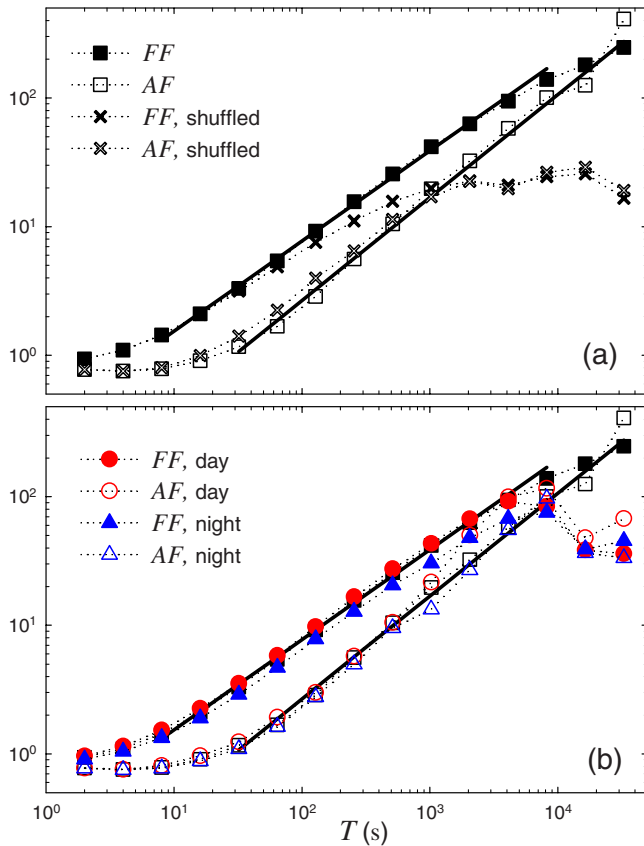


FIG. 8. (Color online) Fano and Allan factors as a function of the counting time-window length T . (a) For comparison, the same analysis over the series of shuffled time intervals is also shown. Solid lines are the results of fits giving slopes $d \approx 0.7$ and $d \approx 0.8$, respectively. (b) Separate analysis for daytime and nighttime data (data are from animal A).

IV. MODELING THE DYNAMICS

The observed super-Poissonian behavior discussed in Sec. III points in the direction of a multiplicative or clustering process, where the occurrence of an event increases the probability of a subsequent one.¹⁴ A class of clustering Poisson process was introduced by Grüneis *et al.*,¹⁵ where there is a primary Poisson process triggering the occurrence of a sequence of events (clusters), each following a secondary Poisson process. In each cluster the number m of events is a random variable.

The statistical properties of this two-stage cascade are determined also by the cluster size distribution $p(m)$. A special case of interest in the context of $1/f^\alpha$ fluctuations is $p(m) \propto 1/m^\eta$ for $m \leq N_0$ and null otherwise. For $3/2 < \eta < 3$, in the limit $N_0 \rightarrow \infty$, it was reported¹⁵ that the exponent of the variance/mean curve is $d = (7 - 2\eta)/4$ while the exponent of the spectral density is $3 - \eta$. If $\eta = 2$, $1/f$ noise is obtained and $d = 3/4$, which is in good accord with the present outcomes. Although the clustering Poisson process of Grüneis *et al.* can reproduce some of the observed scalings, it is not clear how such a cascade process would precisely be originated in the present context.

The same difficulty applies to other fractal or fractal-rate stochastic point processes.¹¹ Recall also that for many processes cited in Ref. 11, solely the distribution of rates is scale-free, while interevent times present a more trivial sta-

tistics. In the present case, however, interevent times are not only scale-free but also present long-range correlations, indicating nonrenewal processes.

It is plausible that animal activity is triggered when some internal dynamical state variable reaches some value. Without being too specific, an animal can move to eat when glucose level reaches some low value, for instance. Of course, biological reality will indicate that nothing in the judgment of the state variable nor in the threshold value can be very precise. Therefore, one can imagine a quantity relaxing toward a fluctuating threshold that resets upon crossing it. Variants of this scenario are very common in the literature where fluctuations are introduced in either the threshold level or in the activation function.¹⁶⁻¹⁹ In particular, we examine here the variant where the threshold fluctuates following a (bounded) Wiener process with diffusion constant D . This version was introduced by Davidsen and Schuster¹⁹ and is closely related to a previously proposed model for $1/f$ noise.²⁰

In Fig. 9(a), we present a representative example of the fluctuating threshold Θ and the relaxation dynamical variable V as functions of time. Figures 9(b)–9(d) show the model dynamics. The distribution of interevent times depends on the specific shape of the decay of $V(t)$, the relaxation process. If the decay has the shape $V(t) = V_2 - K(t - t_{\text{last}})^\kappa$, where t_{last} is the time of the previous adjacent trigger, then the power-law distribution of interevent times has exponent $\mu = 2 - \kappa$.¹⁹ In particular $\kappa = 0.25$ yields $\mu = 1.75$ close to the observed values, and as soon as κ approaches zero (abrupt decay), the exponent can increase up to a value slightly smaller than 2. This relaxation ruled by κ might explain the observation in Ref. 7 of $\mu \sim 1.7$ in depressed individuals and $\mu \sim 1.9$ in control ones. At the same time it is clear that the power law embedded in the model is crucial for replicating the observations; however it will be premature to speculate too much about the precise physiological justification for it. It needs to be noted that the decay can be also seen as resulting from multiple exponentials, such as in the case of diffusion across many barriers.

Besides the interevent time distributions, the other main correlation features seen in the data are reproduced as displayed by the FF and AF measures (notice, though, the relatively larger dip for short T in the AF). It is known that the model dynamics yields $1/f$ spectral properties.¹⁹ We have verified (not shown) that the interevent times are power law correlated and that the distribution of rates is scale-free, as observed for real data, although the exponents are different for the chosen set of parameter values.

Overall, this simple model is able to reproduce the observed phenomenology and it is known to be robust under the addition of noise over the activation signal.¹⁹ Finally, the duration of individual events could also be incorporated easily into the model by an additional integration process consistent with the observed statistics.

V. FINAL OBSERVATIONS

In summary, the results show that animal motion is scale-free in all of the relevant statistics analyzed. It is par-

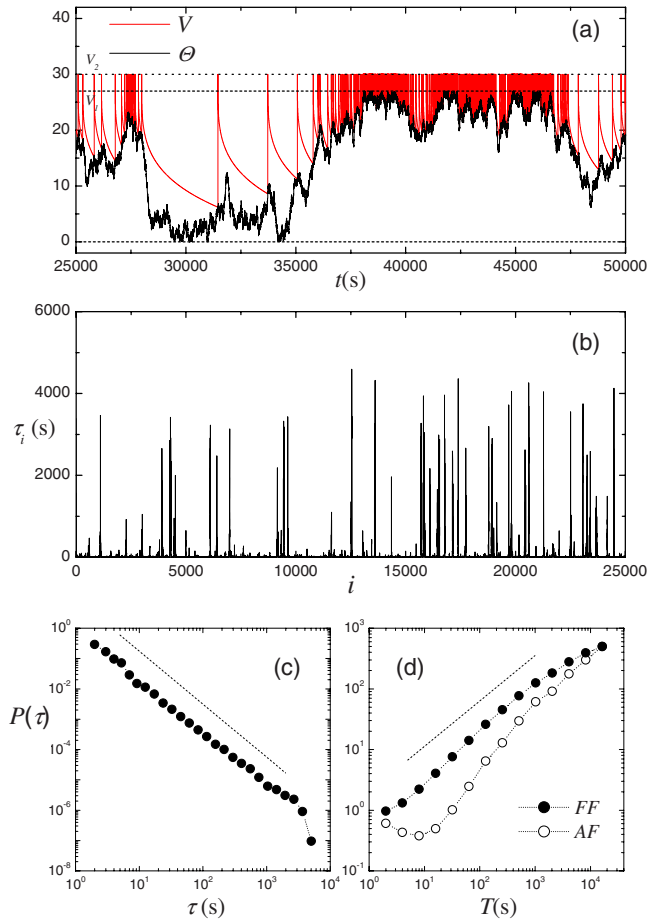


FIG. 9. (Color online) Relaxation toward a fluctuating threshold model. (a) Plots as a function of time of the threshold Θ (black line) that fluctuates diffusively (with coefficient D) between the levels 0 and V_1 (dashed lines); the dynamical variable V (thin red line) that describes the relaxation from the excited level V_2 down to the threshold and is characterized by amplitude K and exponent κ . [(b)–(d)] Results of simulations performed up to time 10^6 in units that correspond to ~ 1 s of real time. Model parameters are $(V_1, V_2, D, K, \kappa) = (27, 30, 0.04, 3.0, 0.25)$. (b) Series of interevent intervals. (c) Distribution of interevent times. Dotted line indicates $\mu = 1.75$. (d) Fano and Allan factors vs counting window length T . Dotted line corresponds to $d = 0.7$.

ticularly clear that the scaling is introduced by the inactivity pauses both by its length as well as by its specific ordering. These results are robust for all animals studied and invariant when day and night data are analyzed separately. While motion episodes do possess a definite time scale and are basically exponentially distributed, the distribution of interevent intervals is scale-free over a broad time scale from a few up to thousands of seconds. Scaling is also demonstrable in the rates of event's occurrence.

The present results resemble those reported for human activity patterns exhibiting similar heavy tailed distributions. However, it is unclear that the explanation given in Ref. 3 for the bursty patterns of human activity could be applied here, given the relative absence of sophisticated cognitive processes in the animals. In other words, the queuing process, attributed to give rise to the power-law tails in humans, hardly can be imagined to intervene in the rat's activity.

It is interesting that human motor activity shows very similar statistics^{6,8} to that demonstrated here. The quantita-

tive aspects for the scaling laws were reported to remain unchanged under usual daily activities or periodic scheduled work. These observations were consistent with earlier results from the study of time series of heartbeat intervals^{13,21,22} from healthy humans. Then, it has prompted the suggestion that multiscale physiological mechanisms are responsible for the observation of these long-term correlated dynamics.⁶ Other related approaches²³ consider that animal motion could be visualized as the output of a large nonlinear dynamical system (e.g., the brain-body-environment ensemble) whose repertoire includes the kind of dynamics observed in these experiments. Finally, the possibility that the complexity of the environment in itself influences animal behavior needs to be carefully considered.²⁴ The fluctuating-threshold dynamics discussed here is biologically plausible and reproduces well the observed rat motor activity. It is possible that appropriate modifications of this model can provide insights on the long-term rhythm alterations observed on individuals with mood disturbances, depression, and other neurological disorders such as chronic pain.

ACKNOWLEDGMENTS

D.R.C. is supported by NIH NINDS of USA, Grant No. NS58661; data collection was supported by NIH NINDS of USA, Grant No. NS42660. C.A. acknowledges Northwestern University for the kind hospitality and Brazilian agencies CNPq and Faperj for partial financial support.

- ¹A. Vazquez, J. G. Oliveira, Z. Dezso, K. I. Goh, I. Kondor, and A.-L. Barabási, *Phys. Rev. E* **73**, 036127 (2006).
- ²A. Vazquez, *Physica A* **373**, 747 (2007).
- ³A.-L. Barabási, *Nature (London)* **435**, 207 (2005).
- ⁴D. B. Stouffer, R. D. Malmgren, and L. A. N. Amaral, e-print arXiv:physics/0510216 and arXiv:physics/0605027; A.-L. Barabási, K.-I. Goh, and A. Vazquez, e-print arXiv:physics/0511186; R. D. Malmgren, D. B. Stouffer, A. E. Motter, and L. A. N. Amaral, *Proc. Natl. Acad. Sci. U.S.A.* **105**, 18153 (2008).
- ⁵C. Anteneodo, R. Dean Malmgren, and D. R. Chialvo, e-print arXiv:0907.1263.
- ⁶K. Hu, P. C. Ivanov, Z. Chen, M. F. Hilton, H. E. Stanley, and S. A. Shea, *Physica A* **337**, 307 (2004).
- ⁷T. Nakamura, K. Kiyono, K. Yoshiuchi, R. Nakahara, Z. R. Struzik, and Y. Yamamoto, *Phys. Rev. Lett.* **99**, 138103 (2007).
- ⁸L. A. N. Amaral, D. J. Bezerra Soares, L. R. da Silva, L. S. Lucena, M. Saito, H. Kumano, N. Aoyagi, and Y. Yamamoto, *Europhys. Lett.* **66**, 448 (2004); K. Ohashi, G. Bleijenberg, S. van der Werf, J. Prins, L. A. N. Amaral, B. H. Natelson, and Y. Yamamoto, *Methods Inf. Med.* **43**, 26 (2004).
- ⁹T. Nakamura, T. Takumi, A. Takano, N. Aoyagi, K. Yoshiuchi, Z. R. Struzik, and Y. Yamamoto, *PLoS ONE* **3**, e2050 (2008).
- ¹⁰Experiments conducted at Northwestern University according to Animal Care and Use Committee regulations.
- ¹¹S. Thurner, S. B. Lowen, M. C. Feurstein, C. Heneghan, H. G. Feichtinger, and M. C. Teich, *Fractals* **5**, 565 (1997).
- ¹²C. A. Hidalgo R., *Physica A* **369**, 877 (2006).
- ¹³C.-K. Peng, J. Mietus, J. M. Hausdorff, S. Havlin, H. E. Stanley, and A. L. Goldberger, *Phys. Rev. Lett.* **70**, 1343 (1993).
- ¹⁴B. E. A. Saleh and M. C. Teich, *Proc. IEEE* **70**, 229 (1982).
- ¹⁵F. Grüneis, M. Nakao, and M. Yamamoto, *Biol. Cybern.* **62**, 407 (1990); F. Grüneis, *Physica A* **123**, 149 (1984); F. Grüneis and H. J. Baiter, *ibid.* **136**, 432 (1986).
- ¹⁶A. M. Wing and A. B. Kristofferson, *Percept. Psychophys.* **13**, 455 (1973).
- ¹⁷G. Schöner, *Brain Cogn.* **48**, 31 (2002) (and references therein).
- ¹⁸E.-J. Wagenmakers, S. Farrell, and R. Ratcliff, *Psychon. Bull. Rev.* **11**, 579 (2004).
- ¹⁹J. Davidsen and H. G. Schuster, *Phys. Rev. E* **65**, 026120 (2002).

- ²⁰B. Kaulakys and T. Meskauskas, [Phys. Rev. E](#) **58**, 7013 (1998).
- ²¹C. Braun, P. Kowallik, A. Freking, D. Haderer, K.-D. Kniffki, and M. Meesmann, [Am. J. Physiol. Heart Circ. Physiol.](#) **275**, H1577 (1998).
- ²²M. Meesmann, J. Boese, D. R. Chialvo, P. Kowallik, W. R. Bauer, W. Peters, F. Grüneis, and K.-D. Kniffki, [Fractals](#) **1**, 312 (1993).
- ²³P. Bak, *How Nature Works* (Oxford University Press, New York, 1997).
- ²⁴D. Boyer, G. Ramos-Fernandez, O. Miramontes, J. L. Mateos, G. Cocho, H. Larralde, H. Ramos, and F. Rojas, [Proc. R. Soc. London, Ser. B](#) **273**, 1743 (2006).